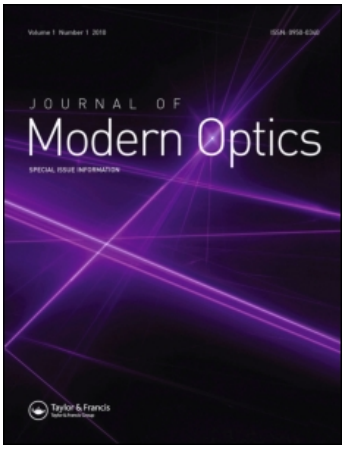

Journal of Modern Optics
Publication details, including instructions for authors and subscription information:
http://www.informaworld.com/smpp/title~content=t713191304

Cone directionality from laser ray tracing in normal and LASIK patients

Susana Marcos[a]; Stephen A. Burns[b]
[a] Instituto de Óptica, Consejo Superior de Investigaciones Científicas, Serrano 121, Madrid 28006, Spain
[b] School of Optometry, Indiana University, Bloomington, IN 47405, USA

First published on: 14 May 2009

To cite this Article Marcos, Susana and Burns, Stephen A.(2009) 'Cone directionality from laser ray tracing in normal and LASIK patients', Journal of Modern Optics, 56: 20, 2181 — 2188, First published on: 14 May 2009 (iFirst)
To link to this Article: DOI: 10.1080/09500340902927074
URL: http://dx.doi.org/10.1080/09500340902927074

Journal of Modern Optics
Vol. 56, No. 20, 20 November 2009, 2181–2188

Taylor & Francis
Taylor & Francis Group

Cone directionality from laser ray tracing in normal and LASIK patients

Susana Marcos[a]* and Stephen A. Burns[b]

[a]*Instituto de Óptica, Consejo Superior de Investigaciones Científicas, Serrano 121, Madrid 28006, Spain;*
[b]*School of Optometry, Indiana University, 800 E. Atwater, Bloomington, IN 47405, USA*

(*Received 30 December 2008; final version received 26 March 2009*)

Laser ray tracing, a technique originally developed to measure ocular aberrations from the deviations of the local ray aberrations as a function of entry pupil, was used to assess cone directionality in 29 normal eyes (seven of which underwent LASIK surgery) and seven eyes after LASIK corneal refractive surgery for myopia. The total intensity of the retinal aerial images was computed as a function of the entry location of the illuminated beam. The measured intensity distribution was fit to a two-dimensional Gaussian function plus a constant background. The maximum of the distribution represents the pupillary location toward which the cone photoreceptors are oriented (peak of the optical Stiles–Crawford, SCE, function). We found the average SCE peak location was located 0.43 ± 0.96 mm nasally and 0.60 ± 0.87 mm inferiorly to the center of the pupil. In general, there was not a relation between the pupillary area of best quality and SCE peak location, either pre-operatively or post-operatively. The cone directionality shape factor was also unchanged by surgery. However, in two eyes, pre- and post-operative SCE peak location changed significantly. LASIK refractive surgery decreased the MTF in all eyes, even when the actual SCE directionality of the subject is considered. In the two eyes that showed significantly different SCE peak location, the apodized post-operative MTF with the post-operative SCE peak exceeded the simulated post-operative MTF assuming no shift in the SCE peak. However, the statistical power of these two cases is low, and the general findings are consistent with the hypothesis that differences in optical quality are not a major driving mechanism for cone orientation.

Keywords: Stiles–Crawford; cone orientation mechanism; ocular aberrations; optical quality; laser ray tracing; LASIK surgery

1. Introduction

Cone photoreceptors exhibit a high degree of directionality. It is well known than most retinal cones point toward a specific pupil location. Light entering the eye close to that location is perceived as brighter than light entering through other pupillary areas. This phenomenon was first observed psychophysically by Stiles and Crawford in 1933, and the inhomogeneous luminous efficiency at the pupil plane is known as the Stiles–Crawford function of the first kind (SCE) [1,2].

Although much of the literature on the SCE effect is based on psychophysical measurement techniques, in recent years, reflectometric techniques have been developed that allow a much more rapid estimation of cone directionality [3–5]. The common principle of the reflectometric techniques is that when the photopigment is bleached part of the light captured by the cones is reflected back through the cone outer segment and redirected toward the pupil. This remitted intensity function is fairly well described by a Gaussian intensity distribution in the pupil conjugate plane. Several reflectometric techniques have been described in the literature for measuring the SCE. These techniques differ in the illumination schemes, including fixed views [4], scanning beam [5], scanning entry and exit pupils [3], in which plane the function is measured (retinal or pupil), and the retinal area sampled (typically between 0.5 and 2 deg). Also the single-entry photoreceptor alignment reflectometric (PAR) technique determines the fitting parameters of the light intensity distribution imaged at the pupil plane, whereas the multiple-entry PAR integrates the light reflected back by the cone photoreceptors from pupillary images [6,7], and determines the fitting parameters of the total intensity as a function of the entry location of the illuminating beam. Measurements from other techniques are based on either of those approaches or a combination of both. One more recent study has reported estimates of cone directionality from resolved individual cone images for different illumination angles [8]. It has been shown that the different techniques (optical and psychophysical) provide similar estimates of the SCE peak (location toward the cones are pointing) [6] although the width of the distribution varies depending on the technique (with psychophysical and multiple-entry PAR techniques providing broader distributions than the

*Corresponding author. Email: susana@io.cfmac.csic.es

ISSN 0950–0340 print/ISSN 1362–3044 online

DOI: 10.1080/09500340902927074
http://www.informaworld.com

single-entry PAR) [7] and experimental conditions (retinal sampled area [7], wavelength [7,9,10], retinal location [11], etc.). In addition, optical coherence tomography has been used to show that the directionality measured using reflectometric techniques arise from both the inner and outer segments of the cones [8].

In the current study we use a laser ray tracing system to measure cone directionality. In this technique, originally developed to measure optical aberrations of the eye [12], a narrow beam of light scans the pupil, as the corresponding aerial image of the retina is captured at a retinal conjugate plane. Ray aberrations are estimated as the centroid deviation of the aerial images with respect to the principal ray. Cone directionality is measured as the variation in the total intensity of the aerial image as a function of entry pupil position. The decrease in the maximum intensity of the retinal aerial images of a point source for eccentric small pupils (2 mm) had been observed before, and attributed primarily to higher amounts of aberration in the pupil periphery [13]. However, to our knowledge, the total intensity of the aerial images with varying entry pupil had never been used to assess cone directionality.

The location of the SCE peak varies markedly between individuals [4,14,15], and this draws into question the mechanism that drives the cone photoreceptors to point to a specific pupillary location. Several studies suggest that the cones would point toward the pupillary aperture (phototropism) as supported from case reports of eccentric SCE peak in a patient with traumatic pupil displacement [16], cone realignment (SCE peak shift) in one subject wearing an opaque contact lens with an eccentric aperture under continuous mydriasis [17], or one subject with congenital cataract and an eccentric clear aperture after cataract removal [18]. Other studies reported unchanged SCE function in one patient after successful recovery from retinal epithelium detachment [19–21]. However, the reasons why, in many subjects, the cones point to pupillary regions typically blocked by the iris, still remain unclear. Burns and Marcos [15] explored possible interactions between optical degradation (wave aberrations) and SCE peak location (measured by PAR). They found that, while in general cone photoreceptors never pointed toward pupillary regions that were optically degraded, they did not point systematically to the least aberrated area of the pupil. In the current investigation, we tested this hypothesis further, by measuring cone directionality (using laser ray tracing) in a group of subjects before and after LASIK corneal surgery (which had significantly altered the wave aberration from its pre-operative distribution) [22,23].

2. Methods

2.1. Subjects

We measured 22 normal eyes (13 OD and 9 OS, from 16 subjects) and seven LASIK eyes, measured pre- and post-operatively (four OD and three OS, from six patients) for a total of 29 eyes in 20 subjects. Refractions in normal and pre-operative eyes ranged from -12 to $+0.75$D (-4.16 ± 3.0D). Subjects' ages ranged from 19.0 to 50.3 (28.6 ± 8.5) years old.

LASIK patients selected are a sub-sample of those patients whose total and ocular aberrations had been previously reported in an earlier study [22,23]. Myopic LASIK had been conducted using a flying spot excimer laser controlled with a standard ablation algorithm (Bausch & Lomb, Technolas Planoscan). Extensive details on the surgery and optical outcomes (including examples of pre- and post-operative wave aberration patterns) can be found in the previous publications [22,23]. Pre-operative measurements were conducted 21 ± 35 days before surgery and post-operative measurements 47 ± 23 days after surgery. The average spherical correction was -5.2 ± 1.7 D before surgery. In the surgical eyes of the present study, high order aberrations increased following surgery by a factor of 1.7, spherical aberration increased by a factor of 2.9, third order aberrations alone by a factor of 1.5, for 6.5 mm pupils.

All subjects were informed on the nature of the study and signed a consent form, which had been approved by the Institutional Review Boards. All experimental protocols followed the tenets of the Declaration of Helsinki.

2.2. Laser ray tracing and experimental protocols

The laser ray tracing (LRT) principle and instrumentation for measuring ocular aberrations have been described in detail in [24–26]. For the purpose of the study the instrument was changed slightly to measure cone directionality.

A 0.4 mm beam (pupil size) sampled a 6.5 mm pupil using a hexagonal sampling pattern configuration. A total of 37 ray entry locations (at 1 mm steps) were used. Aerial images of the retina were simultaneously captured using a cooled CCD camera. We utilized a 532 nm wavelength, to increase the relative cone-photoreceptor reflectance. In addition, a quarter-wave plate was introduced between the beam splitter and the eye, so that only light with the same state of polarization as that of the illuminating beam is collected, as previous studies had shown that light reflected from cone photoreceptors tends to preserve the state of polarization of the incident light (see [4], Bueno, 2001 #1152, and [27,28]). In a previous study

we had shown large differences in the relative intensity of the aerial images collected in a parallel and a cross-polarization configuration [29] using both Hartmann–Shack and LRT as well.

A single measurement lasted approximately 5 s. The power incident on the cornea was 4 μW. Each measurement consisted of five consecutive runs, with a set of 37 aerial images of the retina for each run. While the stimulus used was calculated to have bleached the cones within the first measurement, we tested for this by comparing directionality across the five measurements and found no trend. In general a failure to bleach in the earlier runs would produce a change in both the peak amplitude and the width of directionality [30].

Subjects' pupils were dilated using tropicamide 1%, and their head positions were stabilized with a dental impression and a headrest. The position of the pupil was continuously monitored to ensure proper alignment of the pupil center to the optical axis of the instrument. Spherical refractive errors were corrected with trial lenses when necessary. Additionally to the five test series, a control series of measurements were made where the eye was replaced by a black diffuser, providing a measurement of instrument reflections and instrumental stray light. The control measurements were subtracted from the test images.

2.3. Data processing

Dedicated routines were written in Matlab (Mathworks, Natick, MA) to extract the total intensity of the aerial images and to fit the resulting intensity estimates to Gaussian distributions as a function of pupil entry position. The CCD area subtended a retinal field of 4.95 deg (240 pixels, giving approximately 1.2 arcmin or 6 μm per pixel), with typical width at half maxima of the retinal spot images subtending 10 arcmin. The total intensity of each aerial image was integrated over a circular sub-area of 20 pixels in diameter, centered at the position of its maximum.

The estimated total intensity as a function of entry pupil location is fit with equation [4]:

$$B + I_{\max} 10^{-\rho_s[(x-x_o)^2+(y-y_o)^2]}, \quad (1)$$

where B is a constant that accounts for light diffusely reflected, which does not vary with pupil position, and the second term is a two-dimensional Gaussian function that represents the light directly guided from the photoreceptors; $I_{\max}$ is the intensity at the peak; x_o and y_o are the pupillary coordinates of the peak, and ρ_s is the directionality factor. Fits were obtained both for average intensity data across five consecutive measurements, and for individual measurements. Unpaired Student t-tests were performed to assess possible significant differences (shifts) in the location of the peak before and after LASIK surgery in each patient.

3. Results

3.1. Directionality from LRT measurements: normal eyes

Figure 1 (top row) shows examples from four eyes of the variation in aerial image total intensity for each of the 37 entry locations across the pupil. Each square represents average total intensity across five repeated measurements, and is depicted in the pupillary location of the corresponding entry pupil, on a 6.5 mm pupil diameter. Aerial images corresponding to entry pupils close to the directionality peak are brighter than those corresponding to peripheral entry locations. Figure 1 (bottom row) shows the predicted intensity for the best fit of Equation (1) to the data.

In general, the fitted function represents accurately the measured total intensity (with a variance accounted for by the fit ranging from 96 to 99% across eyes). The pedestal or constant background (B) in Equation (1) is on average 46% of the maximum intensity ($I_{\max}$). The average cone directionality factor (ρ_s) in normal eyes ($n = 29$) is $0.10 \pm 0.06\,\mathrm{mm}^{-2}$.

Figure 2 shows the coordinates of the peak of the total intensity distribution in all normal eyes of the study ($n = 29$). Positive horizontal coordinates represent nasal shifts in right eyes, and temporal shifts in left eyes, and vice versa for negative horizontal coordinates. Positive vertical coordinates represent superior shifts in both right and left eyes. Figure 4(b) (see Section 3.2)

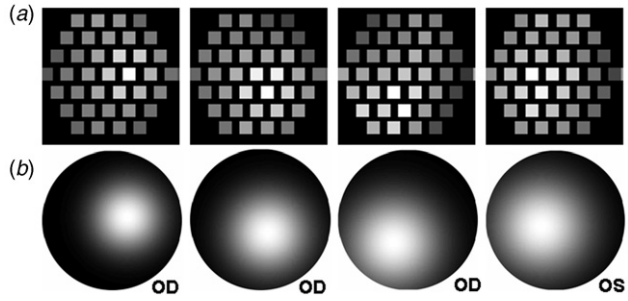

Figure 1. Examples of intensity distributions as a function of entry pupil in four normal eyes. (a) Aerial images total intensity maps. Each small square represents the total intensity of an aerial image of the LRT series, and is depicted at the corresponding laser entry location. (b) 2D Gaussian function fits to the corresponding intensity maps above (minus a background level). The peak of the distribution tends to be shifted nasally both in right (to the right) and left eyes (to the left). Rho values vary from 0.09 to 0.18 mm^{-2} in these four eyes. Pupil diameter is 6.5 mm.

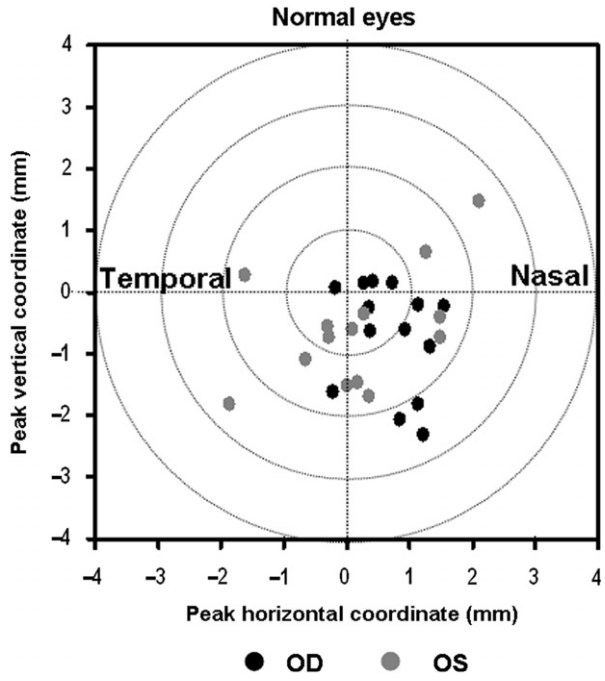

Figure 2. Cone directionality peak location in all normal eyes of the study ($n = 29$). Right eyes are represented by black circles and left eyes by gray circles.

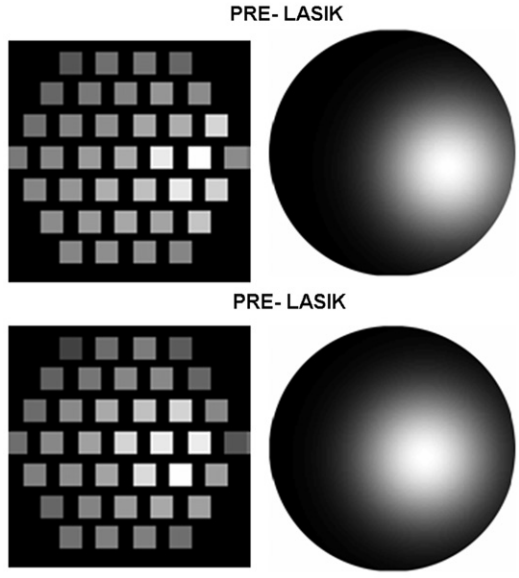

Figure 3. Examples of intensity distributions in an eye (#1, OS) before and after LASIK surgery. Left panels represent the total intensity (computed from the aerial images) as a function of entry location, right panels are the corresponding fit to Gaussian functions. There is no significant shift in the peak of the intensity distribution after the procedure. Pupil diameter is 6.5 mm.

shows examples of five repeated measurements on one eye (for both pre- and post-operative measurements). On average, the standard deviation of the measured peak coordinates is 0.41 and 0.35 mm for the horizontal and vertical direction. The variability is slightly higher than the reported variability of pupil centration (0.17 and 0.11 mm, respectively) in a second-generation LRT system during the course of a measurement [31]. We measured a large intersubject variability in the peak location. Only 34.5% of the eyes have the cone photoreceptors pointing within 1 mm from the pupil center, and 17.2% of the eyes have maxima in cone directionality more than 2 mm from the center of the pupil. On average, the peak location was 0.43 ± 0.96 mm nasally and 0.60 ± 0.87 inferior to the geometric center of the pupil.

3.2. *Cone directionality before and after LASIK*

Figure 3 shows an example of the aerial image total intensity patterns in one eye before (8 days) and after (24 days) LASIK surgery, and the corresponding cone directionality component fitted function. In this eye (#1), the peak is shifted temporally and inferiorly before and after the procedure, and the difference in the peak location pre- and post-operatively is not statistically significant. The cone directionality factor ρ_s was 0.14 mm^{-2} both pre- and post-operatively.

Figure 4(*a*) shows peak locations before (solid symbols) and after (open symbols) LASIK surgery in the seven eyes of the study. Figure 4(*b*) shows peak locations from repeated measurements before (solid symbols) and after (open symbols) LASIK surgery for Eye #7 to illustrate the typical variability of the measurements. The peak coordinates are also represented in Figure 4(*c*) (horizontal, upper panel, and vertical, lower panel). The error bars are standard deviations of individual fits to repeated data. There are no statistically significant differences in the peak location before and after LASIK, except for the peak horizontal coordinate ($p = 0.035$) and vertical coordinate ($p = 0.032$) of Eye #4, and the horizontal coordinate ($p = 0.015$) of Eye #6. The difference in the vector length of the SCE location between pre- and post-operative measurements was only significant in Eye #6 ($p = 0.02$). In the rest of the eyes, the shift between pre- and post-operative peak ranges from 0.23 to 0.61 mm (0.38 ± 0.14 mm) and was not statistically significant ($p > 0.05$). The cone directionality factor did not change significantly either individually or on average ($\rho_{s\text{-PRE}} = 0.133 \pm 0.06$ and $\rho_{s\text{-POST}} = 0.126 \pm 0.04$).

4. Discussion

We have demonstrated that laser ray tracing, which was originally developed to measure ocular wavefront

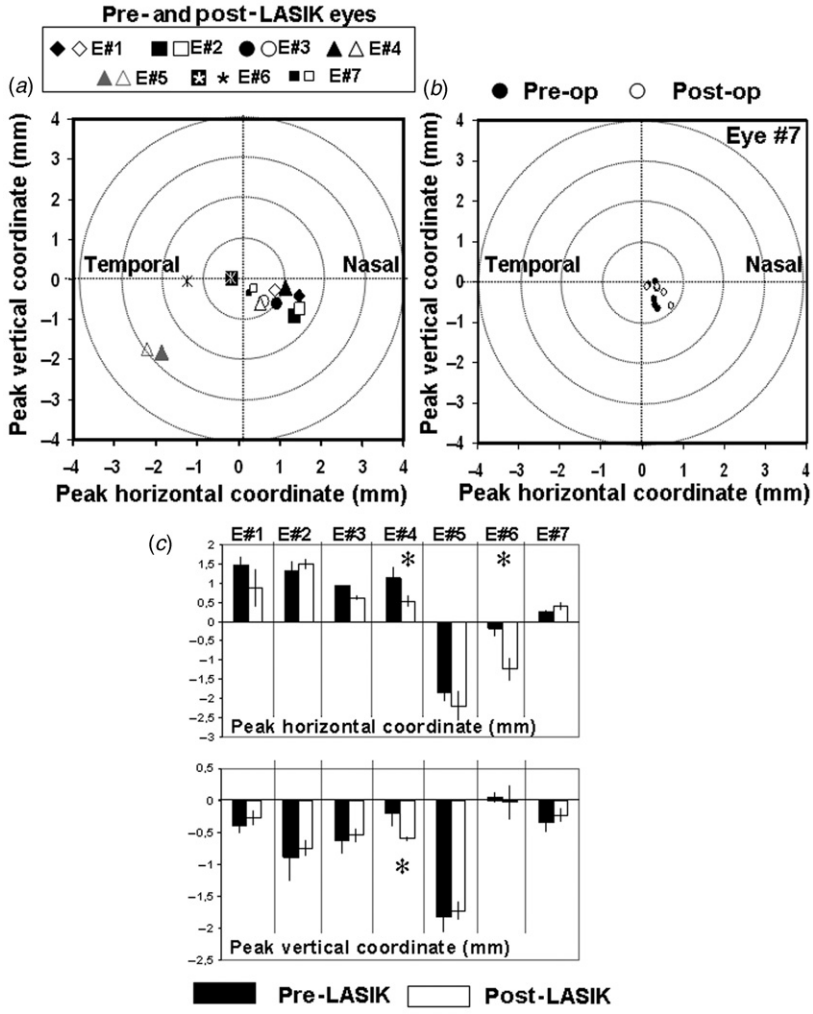

Figure 4. (*a*) Cone directionality peak location in the seven eyes of the study measured before and after LASIK. Each eye is depicted by the same symbol shape. Solid symbols are pre-operative values and open symbols are post-operative values. Black and gray triangles represent right and left eye from the same patient. (*b*) Five repeated measurements of cone directionality peak location in Eye #7 pre-operatively (solid circles) and post-operatively (open circles). (*c*) Bar plot showing horizontal and vertical coordinates of pre- and post-operative cone directionality peak locations in seven eyes. Error bars (standard deviations of estimations from five repeated LRT series). Asterisks show statistically significantly different coordinates.

aberrations, also contains information on the directionality of the cone photoreceptors. The measurements of cone directionality obtained by LRT are similar to those obtained with multiple-entry photoreceptor alignment reflectometry [7], although the measurement is performed at a retinal conjugate rather than pupil conjugate plane. Although we have not performed a systematic comparison of the LRT with other techniques to measure cone directionality, we performed measurements on one subject with LRT and single-entry PAR. Figure 5 shows pupillary intensity distribution maps of light reflected back from the retina, obtained with PAR (upper panels) and fittings from the LRT, as described in the present paper (lower panels). Data are for left and right eye of one of the authors (SB), obtained 41 months apart. In both eyes, there is a significant deviation of the peak of the intensity distribution, slightly nasally and inferiorly (OD) and temporally and inferiorly (OS), as estimated both from PAR and LRT.

The average SCE peak location of the normal eyes of the current study, as measured with LRT, agrees with previous data in the literature, both from reflectometric and psychophysical techniques [4,14,15], and confirms the high intersubject variability in the peak location, the average nasal and inferior shift of the peak with respect to the pupil center, and the presence of individuals with highly displaced functions. While all techniques (single-entry and multiple-entry reflectometric, and psychophysical) have proven to yield similar peak locations, the width of the distribution (cone directionality factor ρ_s) differs across

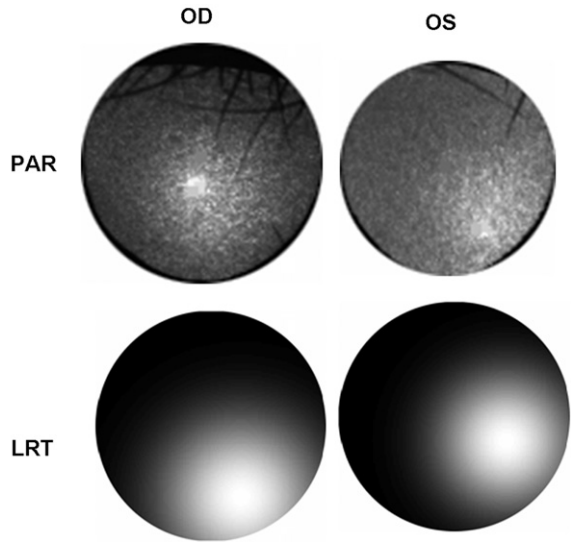

Figure 5. Comparison of pupillary intensity distribution from a photoreceptor alignment reflectometry technique (upper panels) and Gaussian fits to aerial image total intensity distribution from LRT (lower panels) on the right and left eye of a subject measured with both techniques. Pupil diameter is the largest under dilation from PAR and 6.5 mm for LRT. Peak locations (horizontal/vertical coordinates) are (0.23, −1.62) and (1.95, −2.05) from PAR, for OD and OS, respectively. Peak locations (horizontal/vertical coordinates) are (0.86, −2.06) and (1.49, −0.74) from LRT, for OD and OS, respectively.

techniques, with ρ_s estimates from psychophysical techniques typically lower (broader functions) than reflectometric [6]. We found that the LRT cone directionality factor (ρ_s) was on average more similar to single-entry than multiple-entry PAR, although it consists of a multiple-entry technique. These estimates also showed high intersubject variability, as in single-entry PAR and unlike multiple-entry PAR. The intersubject variability may be attributable to the reported variability in foveal cone sizes [32–34] as well as due to changes in the fovea with age [35,36]. In general, smaller diameter cones should produce a broader distribution [6,7]. We did not find this. While the reason is not clear, one possibility is that the small movements of our measurement spot produces a differential contribution from the foveal pit reflection compared to a broader field [37] or perhaps the intensity distribution may be slightly altered by the presence of diffused reflections from anterior segment structures. However, these diffuse reflections are minimized in the maxwellian view and small specular reflection configuration of PAR, and by the limitation of the intensity computation to a small area around the aerial image peak – mimicking a confocal aperture – for the LRT. None of these is expected to alter the estimated cone directionality peak.

The advantage of this combined approach is that the LRT provides simultaneous estimates of the ocular wavefront aberrations as well as cone directionality and has been able to provide combined measurements both pre- and post-LASIK refractive surgery for myopia. While the wave aberration pattern changed dramatically with the procedure (and high order aberrations such as spherical aberration and coma increased significantly) we did not find that the cone orientation shifted with the procedure (except in both coordinates for one eye, and the horizontal coordinate in another eye). In a previous study, we have explored potential relationships between the area of best optical quality in the pupil and cone orientation. We used a similar approach to evaluate optical degradation across the pupil pre- and post-operatively, and to compare the areas of best optics with SCE peak location. Figure 6 shows pupillary maps in all eyes before and after LASIK surgery, computed as the Strehl ratio (for 2 mm pupils, in 0.25 mm steps) across the pupil. The pupillary area of best optical quality changes significantly with the procedure, while the SCE peak remains unchanged in most cases. As previously observed, there is in general no correspondence between the maximum of the optical quality pupillary maps and the SCE peak. Cone directionality (width of the distribution, typically associated with the degree of alignment) did not change with the procedure either. This finding confirms the stability of cone orientation (which case reports had shown to occur even after some retinal processes, such as retinal detachment, had resolved [19–21]). It also demonstrates that, in most eyes, changes in the optical quality of the eye do not result in changes in the cone orientation. Only for two eyes the SCE peak location was significantly different pre- and post-operatively. In these two cases, we explored the apodization effect of the SCE function in the pre- and post-operative modulation transfer function (MTF). Computations were performed for 6.5 mm pupil diameter and a constant shape factor of 0.1 mm^{-2}, assuming the same (pre-op) SCE function pre- and post-operatively and the post-op SCE function. Results are shown in Figure 7, in terms of MTFs, and modulation at a specific spatial frequency (10 c deg^{-1}) in the inset. As previously reported there is a decrease of the MTF after LASIK (by a factor of 1.31, on average across eyes and spatial frequencies, 0 to 60 c deg^{-1}). However, the new SCE location improves the post-operative MTF slightly (by a factor of 1.12, on average). The significant difference in the SCE location (pre- and post-operative) and the improvement of the MTF by a shifted SCE function occurs only in two eyes and does not seem to be the general situation. In fact, no correlation was found between the region of best optical quality in the pupil and cone orientation. This result further supports

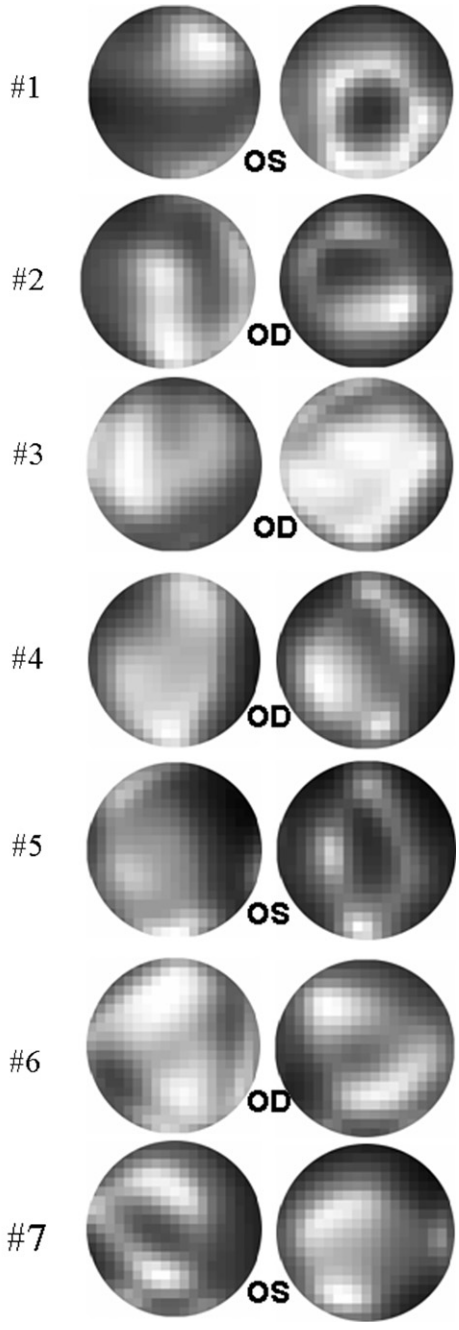

Figure 6. Pupillary Strehl maps computed as the Strehl value for a 2 mm pupil scanned across the pupil at 0.25 mm steps (for astigmatism and third and higher order aberrations), for all eyes pre-operatively (left column) and post-operatively (right column). In most eyes the areas of best optical quality change with surgery. In general, there is no correspondence between the area of best optical quality and cone directionality peak (see Figure 4 for peak coordinates in each eye).

the hypothesis that optical degradation (i.e. orientation toward the best optical pupillary areas, or avoidance of optically degraded areas) is not a driving mechanism for cone orientation [15].

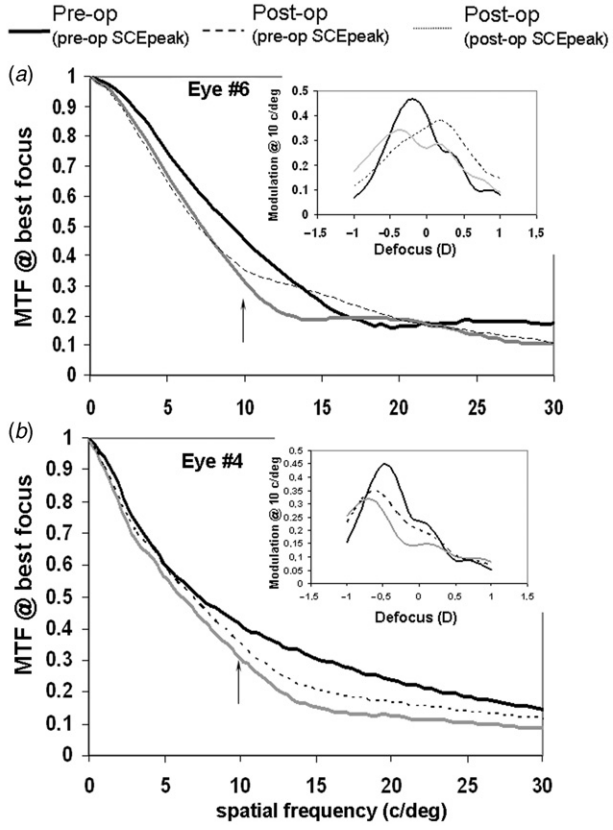

Figure 7. Pre- (black) and post-operative (gray and dashed) modulation transfer function (MTF) at best focus, apodized by the cone directionality function ($\rho = 0.1\,\mathrm{mm}^{-2}$), using the pre-operative SCE peak (black and gray) and the post-operative SCE peak (dashed). The inset represents the through-focus modulation at a spatial frequency of $10\,\mathrm{c\,deg}^{-1}$, marked by an arrow in the MTF plot. Data for the only two eyes that had significantly different pre- and post-operative cone directionality peak locations. (*a*) Eye #6; and (*b*) Eye #4. Pre-operative MTF exceeds the post-operative MTF at all spatial frequencies (and for defocus range of at least 1.5D). The actual post-operative SCE function improves the MTF with respect to that calculated using the pre-operative SCE peak.

Acknowledgements

This work was supported by EURYI-05-102-ES (EUROHORCS-ESF) and FIS2008-02065 (Spanish Ministry of Science and Innovation) to SM; EYO4395 to SB.

References

[1] Stiles, W.S. *Proc. Roy. Soc. (Biol.)* **1939,** *127,* 64–105.
[2] Westheimer, G. *Proc. Biol. Sci.* **2008,** *275,* 2777–2786.
[3] Gorrand, J.M.; Delori, F.C. *Vision Res.* **1995,** *35,* 999–1010.
[4] Burns, S.A.; Wu, S.; Delori, F.; Elsner, A.E. *J. Opt. Soc. Am. A* **1995,** *12,* 2329–2338.

[5] Delint, P.J.; Berendschot, T.T.J.M.; Norren, D. *Vision Res*. **1997,** *37,* 243–248.
[6] He, J.C.; Marcos, S.; Burns, S.A. *J. Opt. Soc. Am. A* **1999,** *16,* 2363–2369.
[7] Marcos, S.; Burns, S.A. *J. Opt. Soc. Am. A* **1999,** *16,* 995–1004.
[8] Gao, W.H.; Cense, B.; Zhang, Y.; Jonnal, R.S.; Miller, D.T. *Opt. Express* **2008,** *16,* 6486–6501.
[9] Choi, S.S.; Doble, N.; Lin, J.; Christou, J.; Williams, D.R. *J. Opt. Soc. Am. A – Opt. Image Sci. Vision* **2005,** *22,* 2598–2605.
[10] Zagers, N.P.A.; Berendschot, T.; van Norren, D. *J. Opt. Soc. Am. A – Opt. Image Sci. Vision* **2003,** *20,* 18–23.
[11] Burns, S.A.; Wu, S.; He, J.C.; Elsner, A.E. *J. Opt. Soc. Am. A* **1997,** *14,* 2033–2040.
[12] Navarro, R.; Losada, M.A. *Optom. Vision Sci*. **1997,** *74,* 540–547.
[13] Artal, P.; Marcos, S.; Iglesias, I.; Green, D.G. *Vision Res*. **1996,** *6,* 3575–3586.
[14] Applegate, R.A.; Lakshminarayanan, V. *J. Opt. Soc. Am. A* **1993,** *10,* 1611–1623.
[15] Marcos, S.; Burns, S.A. *Vision Res*. **2000,** *40,* 2437–2447.
[16] Bonds, A.B.; MacLeod, D.I.A. *Invest. Ophthalmol. Visual Sci*. **1978,** *17,* 754–761.
[17] Applegate, R.A.; Bonds, A.B. *Invest. Ophthalmol. Visual Sci*. **1981,** *21,* 869–873.
[18] Smallman, H.; MacLeod, D.; Doyle, P. *Nature* **2001,** *412,* 604–605.
[19] Enoch, J.M.; Van Loo, J.A.; Okun, E. *Invest. Ophthalmol. Visual Sci*. **1973,** *12,* 849–853.
[20] Smith, V.C.J.; Pokorny, J.; Diddie, K.R. *Mod. Probl. Opthalmol*. **1978,** *19,* 284–295.
[21] Rynders, M.C.; Grosvenor, T.; Enoch, J.M. *Optom. Vision Sci*. **1995,** *72,* 177–185.
[22] Moreno-Barriuso, E.; Merayo-Lloves, J.; Marcos, S.; Navarro, R.; Llorente, L.; Barbero, S. *Invest. Ophthalmol. Visual Sci*. **2001,** *42,* 1396–1403.
[23] Marcos, S.; Barbero, B.; Llorente, L.; Merayo-Lloves, J. *Invest. Ophthalmol. Visual Sci*. **2001,** *42,* 3349–3356.
[24] Moreno-Barriuso, E.; Marcos, S.; Navarro, R.; Burns, S.A. *Optom. Vision Sci*. **2001,** *78,* 152–156.
[25] Llorente, L.; Diaz-Santana, L.; Lara-Saucedo, D.; Marcos, S. *Optom. Vision Sci*. **2003,** *80,* 26–35.
[26] Llorente, L.; Barbero, S.; Cano, D.; Dorronsoro, C.; Marcos, S. *J. Vision*. **2004,** *4,* 288–298.
[27] Van Blokland, G.J. *J. Opt. Soc. Am. A* **1985,** *2,* 72–75.
[28] Brink, H.B.K.; Vanblokland, G.J. *J. Opt. Soc. Am. A – Opt. Image Sci. Vision* **1988,** *5,* 49–57.
[29] Marcos, S.; Díaz-Santana, L.; Llorente, L.; Dainty, C. *J. Opt. Soc. Am. A* **2002,** *19,* 1063–1072.
[30] Prieto, P.M.; McLellan, J.S.; Burns, S.A. *Vision Res*. **2005,** *45,* 1957–1965.
[31] Llorente, L.; Marcos, S.; Dorronsoro, C.; Burns, S. *J. Opt. Soc. Am. A* **2007,** *24,* 2783–2796.
[32] Curcio, C.A.; Sloan, K.R.; Packer, O.; Hendrickson, A.E.; Kalina, R.E. *Science* **1987,** *236,* 579–582.
[33] Williams, D.R. *Vision Res*. **1987,** *28,* 433–454.
[34] Marcos, S.; Navarro, R.; Artal, P. *J. Opt. Soc. Am. A* **1996,** *13,* 897–905.
[35] Eisner, A.; Fleming, S.A.; Klein, M.L.; Mauldin, W.M. *Invest. Ophthalmol. Visual Sci*. **1987,** *28,* 1824–1831.
[36] Elsner, A.E.; Berk, L.; Burns, S.A.; Rosenberg, P.R. *J. Opt. Soc. Am. A – Opt. Image Sci. Vision* **1988,** *5,* 2106–2112.
[37] Williams, D.R. *Invest. Ophthalmol. Visual Sci*. **1980,** *19,* 653–667.